The status of the inflationary paradigm
– A cosmological perspective –

L. Sriramkumar

Department of Physics, Indian Institute of Technology Madras, Chennai

Joint Astro and Particle Physics Meeting

Centre for Gravitational Physics and Astronomy

IUCAA and IISER Pune

February 25, 2018

Plan of the talk

Plan of the talk

The resolution of the horizon problem in inflation

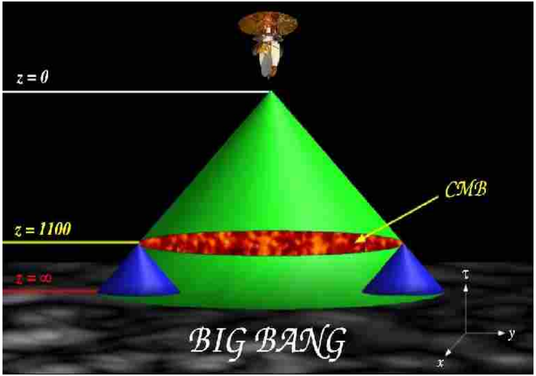

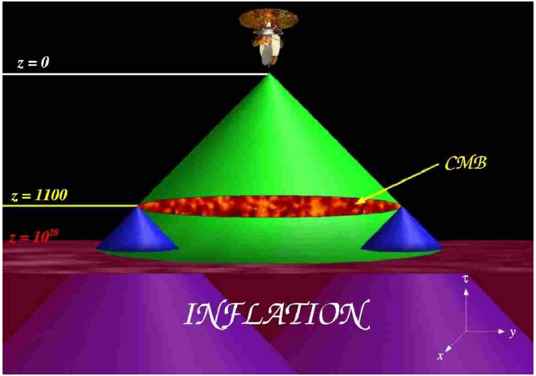

Left: The radiation from the CMB arriving at us from regions separated by more than the Hubble radius at the last scattering surface (which subtends an angle of about 1° today) could not have interacted before decoupling.

[1] Images from W. Kinney, astro-ph/0301448.

The resolution of the horizon problem in inflation

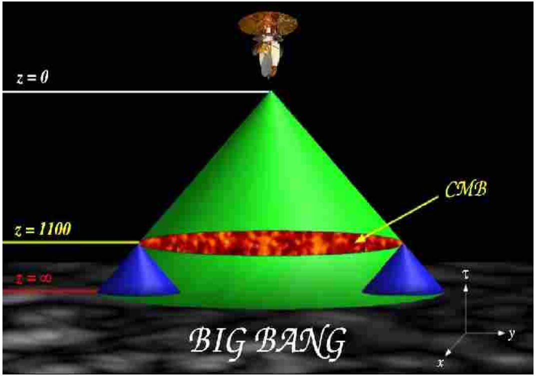

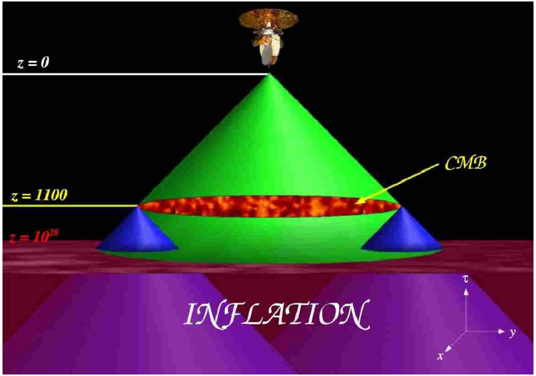

Left: The radiation from the CMB arriving at us from regions separated by more than the Hubble radius at the last scattering surface (which subtends an angle of about 1° today) could not have interacted before decoupling.
Right: An illustration of how an early and sufficiently long epoch of inflation helps in resolving the horizon problem[1].

[1] Images from W. Kinney, astro-ph/0301448.

Bringing the modes inside the Hubble radius

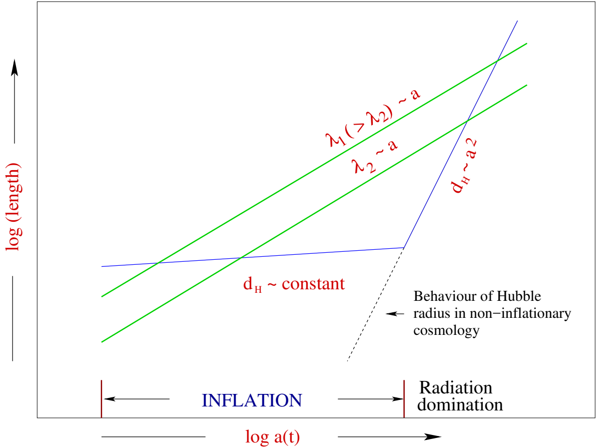

The behavior of the physical wavelength $\lambda_{\rm P} \propto a$ (the green lines) and the Hubble radius H^{-1} (the blue line) during inflation and the radiation dominated epochs[2].

[2]See, for example, E. W. Kolb and M. S. Turner, *The Early Universe* (Addison-Wesley Publishing Company, New York, 1990), Fig. 8.4.

The time and duration of inflation

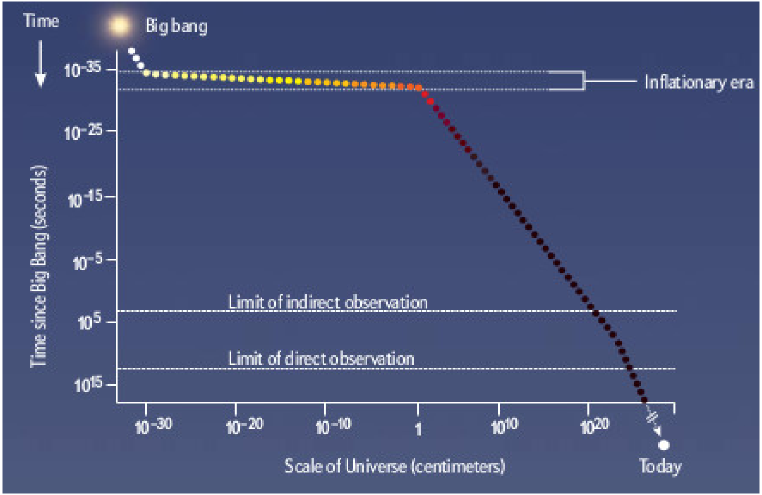

Inflation – a brief period of accelerated expansion – is expected to have taken place during the very early stages of the universe[3].

[3] Image from P. J. Steinhardt, Sci. Am. **304**, 18 (2011).

Driving inflation with scalar fields

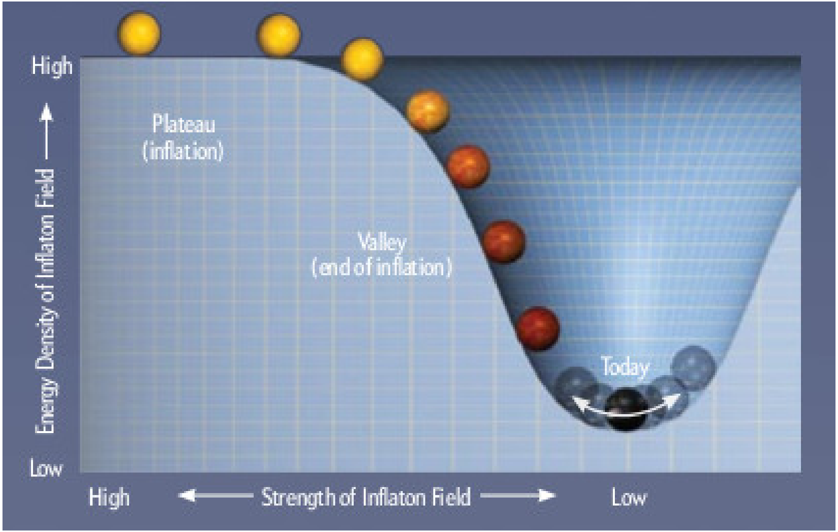

Inflation can be achieved easily with scalar fields encountered in high energy physics[4].

[4] Image from P. J. Steinhardt, Sci. Am. **304**, 34 (2011).

A variety of potentials to choose from

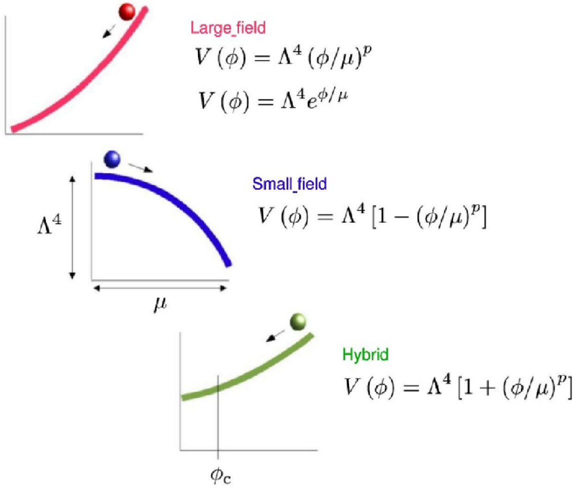

A variety of scalar field potentials have been considered to drive inflation[5]. Often, these potentials are classified as small field, large field and hybrid models.

[5] Image from W. Kinney, astro-ph/0301448.

Constraining inflationary models

5-dimensional assisted inflation
anisotropic brane inflation
anomaly-induced inflation
assisted inflation
assisted chaotic inflation
boundary inflation
brane inflation
brane-assisted inflation
brane gas inflation
brane-antibrane inflation
braneworld inflation
Brans-Dicke chaotic inflation
Brans-Dicke inflation
bulky brane inflation
chaotic hybrid inflation
chaotic inflation
chaotic new inflation
D-brane inflation
D-term inflation
dilaton-driven inflation
dilaton-driven brane inflation
double inflation
double D-term inflation
dual inflation
dynamical inflation
dynamical SUSY inflation
eternal inflation
extended inflation
extended open inflation
extended warm inflation
extra dimensional inflation
F-term inflation
F-term hybrid inflation
false vacuum inflation
false vacuum chaotic inflation
fast-roll inflation
first order inflation
gauged inflation
generalised inflation
generalized assisted inflation
generalized slow-roll inflation
gravity driven inflation
Hagedorn inflation
higher-curvature inflation
hybrid inflation
hyperextended inflation
induced gravity inflation
induced gravity open inflation
intermediate inflation
inverted hybrid inflation
isocurvature inflation
K inflation
kinetic inflation
lambda inflation
large field inflation
late D-term inflation
late-time mild inflation
low-scale inflation
low-scale supergravity inflation
M-theory inflation
mass inflation
massive chaotic inflation
moduli inflation
multi-scalar inflation
multiple inflation
multiple-field slow-roll inflation
multiple-stage inflation
natural inflation
natural Chaotic inflation
natural double inflation
natural supergravity inflation
new inflation
next-to-minimal supersymmetric hybrid inflation
non-commutative inflation
non-slow-roll inflation
nonminimal chaotic inflation
old inflation
open hybrid inflation
open inflation
oscillating inflation
polynomial chaotic inflation
polynomial hybrid inflation
power-law inflation
pre-Big-Bang inflation
primary inflation
primordial inflation
quasi-open inflation
quintessential inflation
R-invariant topological inflation
rapid asymmetric inflation
running inflation
scalar-tensor gravity inflation
scalar-tensor stochastic inflation
Seiberg-Witten inflation
single-bubble open inflation
spinodal inflation
stable starobinsky-type inflation
steady-state eternal inflation
steep inflation
stochastic inflation
string-forming open inflation
successful D-term inflation
supergravity inflation
supernatural inflation
superstring inflation
supersymmetric hybrid inflation
supersymmetric inflation
supersymmetric topological inflation
supersymmetric new inflation
synergistic warm inflation
TeV-scale hybrid inflation

A partial list of inflationary models[6]. The goal is to rule out as many of the models as possible. Until either the cosmic neutrino background or the stochastic gravitational wave background is observed, it is the anisotropies in the CMB that provides the primary window to probe physics operating at the highest energy scales.

[6] From E. P. S. Shellard, *The future of cosmology: Observational and computational prospects*, in *The Future of Theoretical Physics and Cosmology*, Eds. G. W. Gibbons, E. P. S. Shellard and S. J. Rankin (Cambridge University Press, Cambridge, England, 2003).

Plan of the talk

Perturbations induced by quantum fluctuations

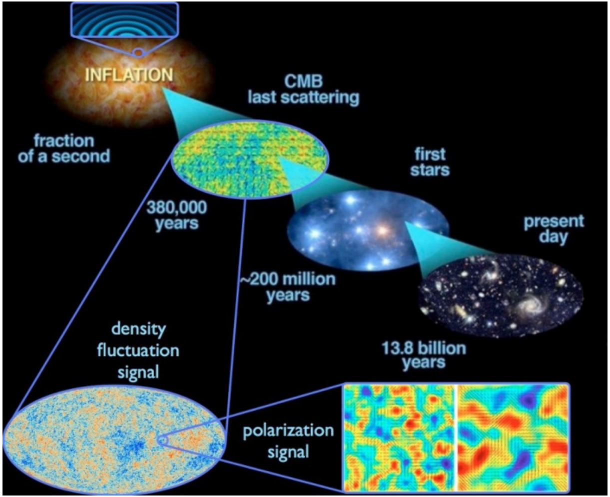

It is the quantum fluctuations associated with the scalar fields that generate the primordial perturbations which, in turn, induce the anisotropies in the CMB

The slow roll scalar amplitude, index and running[7]

At the leading order in the slow roll approximation, the spectral amplitude of the curvature perturbation can be expressed in terms of the potential $V(\phi)$ as follows:

$$\mathcal{P}_{\rm S}(k) \simeq \frac{1}{12\,\pi^2\,M_{\rm Pl}^6}\,\left(\frac{V^3}{V_\phi^2}\right)_{k=a\,H},$$

with the subscript on the right hand side indicating that the quantity has to be evaluated when the modes leave the Hubble radius.

At the same order of the approximation, the scalar spectral index is given by

$$n_{\rm S} \equiv 1 + \left(\frac{{\rm d}\ln \mathcal{P}_{\rm S}}{{\rm d}\ln k}\right)_{k=a\,H} = 1 - 2\,\epsilon_1 - \epsilon_2\,,$$

while the running of the scalar spectral index can be evaluated to be

$$\alpha_{\rm S} \equiv \left(\frac{{\rm d}\,n_{\rm S}}{{\rm d}\ln k}\right)_{k=a\,H} = -\,(2\,\epsilon_1\,\epsilon_2 + \epsilon_2\,\epsilon_3)\,.$$

[7]See, for instance, B. A. Bassett, S. Tsujikawa and D. Wands, Rev. Mod. Phys. **78**, 537 (2006).

The tensor amplitude, spectral index and running

At the leading order in the slow roll approximation, the tensor amplitude is given by

$$\mathcal{P}_{\rm T}(k) \simeq \frac{2}{3\,\pi^2}\,\left(\frac{V}{M_{\rm Pl}^4}\right)_{k=a\,H},$$

while the spectral index and the running can be estimated to be[8]

$$n_{\rm T} \equiv \left(\frac{{\rm d}\,\ln \mathcal{P}_{\rm T}}{{\rm d}\,\ln k}\right)_{k=a\,H} = -2\,\epsilon_1 \quad \text{and} \quad \alpha_{\rm T} \equiv \left(\frac{{\rm d}\,n_{\rm T}}{{\rm d}\,\ln k}\right)_{k=a\,H} = -2\,\epsilon_1\,\epsilon_2.$$

The tensor-to-scalar ratio is then given by

$$r \equiv \frac{\mathcal{P}_{\rm T}(k)}{\mathcal{P}_{\rm S}(k)} \simeq 16\,\epsilon_1 = -8\,n_{\rm T},$$

with the last equality often referred to as the consistency relation[9].

[8] See, B. A. Bassett, S. Tsujikawa and D. Wands, Rev. Mod. Phys. **78**, 537 (2006).

[9] J. E. Lidsey, A. R. Liddle, E. W. Kolb and E. J. Copeland, Rev. Mod. Phys. **69**, 373 (1997).

Plan of the talk

Theoretical angular power spectra[10]

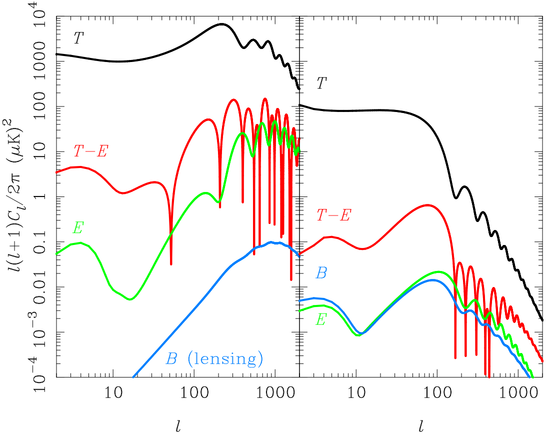

The *theoretically* computed, CMB angular power and cross-correlation spectra – temperature (T, in black), E (in green), B (in blue), and T-E (in red) – arising due to scalars (on the left) and tensors (on the right) corresponding to a tensor-to-scalar ratio of $r = 0.24$. The B-mode spectrum induced by weak gravitational lensing has also been shown (in blue) in the panel on the left.

[10] Figure from A. Challinor, arXiv:1210.6008 [astro-ph.CO].

CMB TT angular power spectrum from Planck

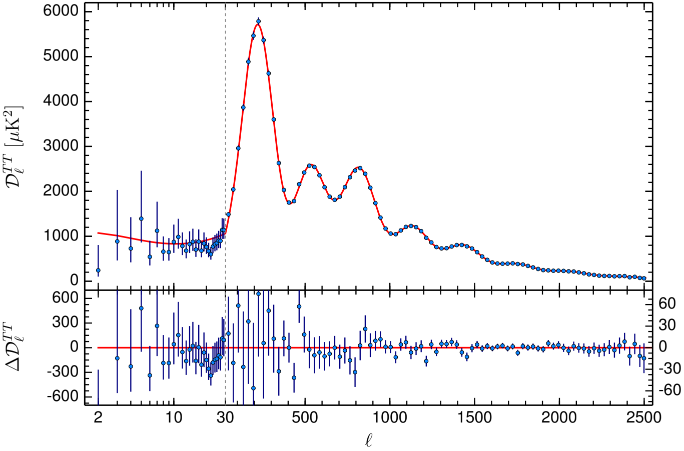

The CMB TT angular power spectrum from the Planck 2015 data (the blue dots with error bars) and the theoretical, best fit ΛCDM model with a power law primordial spectrum (the solid red curve)[11].

[11] Planck Collaboration (P. A. R. Ade *et al.*), Astron. Astrophys. **594**, A20 (2016).

CMB TE and EE angular power spectra from Planck

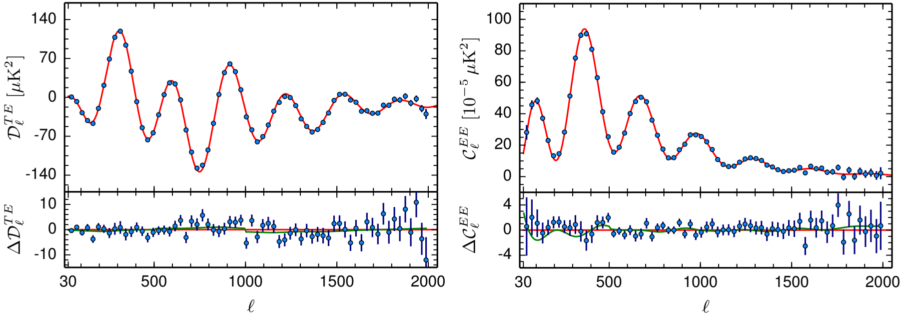

The CMB TE (on the left) and EE (on the right) angular power spectra from the Planck 2015 data (the blue dots with error bars) and the theoretical, best fit ΛCDM model with a power law primordial spectrum (the solid red curves)[12].

[12] Planck Collaboration (P. A. R. Ade *et al.*), Astron. Astrophys. **594**, A20 (2016).

[13] D. N. Spergel and M. Zaldarriaga, Phys. Rev. Lett. **79**, 2180 (1997).

CMB TE and EE angular power spectra from Planck

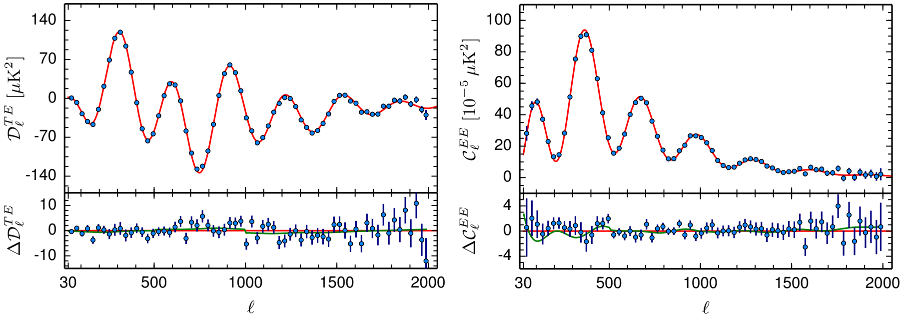

The CMB TE (on the left) and EE (on the right) angular power spectra from the Planck 2015 data (the blue dots with error bars) and the theoretical, best fit ΛCDM model with a power law primordial spectrum (the solid red curves)[12].

The large angle ($50 < \ell < 150$) TE anti-correlation detected by Planck (and earlier by WMAP) is a distinctive signature of primordial, super-Hubble, adiabatic perturbations[13].

[12] Planck Collaboration (P. A. R. Ade *et al.*), Astron. Astrophys. **594**, A20 (2016).

[13] D. N. Spergel and M. Zaldarriaga, Phys. Rev. Lett. **79**, 2180 (1997).

Joint constraints on r and $n_{\rm s}$

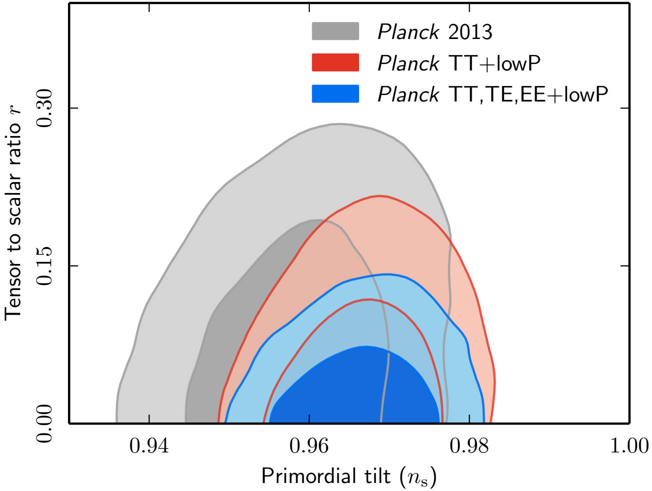

Marginalized joint confidence contours for $(n_{\rm s}, r)$, at the $68\,\%$ and $95\,\%$ CL, in the presence of running of the spectral indices[14].

[14] Planck Collaboration (P. A. R. Ade *et al.*), Astron. Astrophys. **594**, A20 (2016).

Specific inflationary models of interest I

Power law potentials: In power law potentials of the following form[15]:

$$V(\phi) = \lambda\, M_{\rm Pl}^4\, \left(\phi/M_{\rm Pl}\right)^n,$$

inflation occurs for large values of the field, *i.e.* $\phi > M_{\rm Pl}$.

[15] A. D. Linde, Phys. Lett. B **129**, 177 (1983).

[16] L. Boubekeur and D. Lyth, JCAP **0507**, 010 (2005).

[17] K. Freese, J. .A. Frieman and A. V. Olinto, Phys. Rev. Lett. **65**, 3233 (1990).

Specific inflationary models of interest I

Power law potentials: In power law potentials of the following form[15]:

$$V(\phi) = \lambda\, M_{\rm Pl}^4\, (\phi/M_{\rm Pl})^n\,,$$

inflation occurs for large values of the field, *i.e.* $\phi > M_{\rm Pl}$.

Hilltop models: The hilltop models are described by the potential[16]:

$$V(\phi) \simeq \Lambda^4\, [1 - (\phi/\mu)^p + \ldots]$$

and, in these models, the inflaton rolls away from an unstable equilibrium. The ellipsis indicates higher order terms that are considered to be negligible during inflation, but ensure positiveness of the potential.

[15] A. D. Linde, Phys. Lett. B **129**, 177 (1983).

[16] L. Boubekeur and D. Lyth, JCAP **0507**, 010 (2005).

[17] K. Freese, J. .A. Frieman and A. V. Olinto, Phys. Rev. Lett. **65**, 3233 (1990).

Specific inflationary models of interest I

Power law potentials: In power law potentials of the following form[15]:

$$V(\phi) = \lambda\, M_{\rm Pl}^4\, \left(\phi/M_{\rm Pl}\right)^n,$$

inflation occurs for large values of the field, *i.e.* $\phi > M_{\rm Pl}$.

Hilltop models: The hilltop models are described by the potential[16]:

$$V(\phi) \simeq \Lambda^4\, \left[1 - (\phi/\mu)^p + \ldots\right]$$

and, in these models, the inflaton rolls away from an unstable equilibrium. The ellipsis indicates higher order terms that are considered to be negligible during inflation, but ensure positiveness of the potential.

Natural inflation: In natural inflation, a non-perturbative shift symmetry is invoked to suppress radiative corrections, leading to the periodic potential[17]

$$V(\phi) = \Lambda^4\, \left[1 + \cos\left(\phi/f\right)\right],$$

where f is the scale which determines the curvature of the potential.

[15] A. D. Linde, Phys. Lett. B **129**, 177 (1983).

[16] L. Boubekeur and D. Lyth, JCAP **0507**, 010 (2005).

[17] K. Freese, J. .A. Frieman and A. V. Olinto, Phys. Rev. Lett. **65**, 3233 (1990).

Specific inflationary models of interest II

R^2 inflation: The first inflationary model proposed with the action[18]

$$S[g_{\mu\nu}] = \frac{M_{\rm Pl}^2}{2}\int {\rm d}^4x\,\sqrt{-g}\,\left(R + \frac{R^2}{6\,M^2}\right),$$

corresponds to the following potential in the Einstein frame:

$$V(\phi) = \Lambda^4\,\left(1 - {\rm e}^{-\sqrt{2/3}\,\phi/M_{\rm Pl}}\right)^2.$$

---

[18] A. A. Starobinsky, Phys. Lett. B **91**, 99 (1980).

[19] See, for example, R. Kallosh, A. D. Linde and D. Roest, JHEP **1311**, 198 (2013).

Specific inflationary models of interest II

R^2 inflation: The first inflationary model proposed with the action[18]

$$S[g_{\mu\nu}] = \frac{M_{\rm Pl}^2}{2} \int {\rm d}^4x\, \sqrt{-g}\, \left(R + \frac{R^2}{6\, M^2}\right),$$

corresponds to the following potential in the Einstein frame:

$$V(\phi) = \Lambda^4\, \left(1 - {\rm e}^{-\sqrt{2/3}\,\phi/M_{\rm Pl}}\right)^2.$$

α-attractors: A class of inflationary models motivated by recent developments in conformal symmetry and supergravity correspond to the potential[19]

$$V(\phi) = \Lambda^4\, \left[1 - {\rm e}^{-\sqrt{2/3}\,\phi/(\sqrt{\alpha}\, M_{\rm Pl})}\right]^2.$$

A second class of models, called the super-conformal α-attractors, are described by the following potential:

$$V(\phi) = \Lambda^4\, \tanh^{2\,m}\left(\phi/\sqrt{6\,\alpha\, M_{\rm Pl}}\right).$$

[18] A. A. Starobinsky, Phys. Lett. B **91**, 99 (1980).

[19] See, for example, R. Kallosh, A. D. Linde and D. Roest, JHEP **1311**, 198 (2013).

Accounting for post-inflationary evolution

The uncertainties post-inflation are modeled by two parameters: the energy scale $\rho_{\rm th}$ by which the universe has thermalized, and the parameter $w_{\rm int}$ which characterizes the effective equation of state between the end of inflation and the energy scale specified by $\rho_{\rm th}$.

[20] A. R. Liddle and S. M. Leach, Phys. Rev. D **68**, 103503, (2003); J. Martin and C. Ringeval, Phys. Rev. D **82**, 023511 (2010).

Accounting for post-inflationary evolution

The uncertainties post-inflation are modeled by two parameters: the energy scale $\rho_{\rm th}$ by which the universe has thermalized, and the parameter $w_{\rm int}$ which characterizes the effective equation of state between the end of inflation and the energy scale specified by $\rho_{\rm th}$.

The number of e-folds to the end of inflation is described by the expression[20]

$$N_\ast \approx 67 - \ln\left(\frac{k_\ast}{a_0\, H_0}\right) + \frac{1}{4}\,\ln\left(\frac{V_\ast^2}{M_{\rm Pl}^4\,\rho_{\rm end}}\right) + \frac{1-3\,w_{\rm int}}{12\,(1+w_{\rm int})}\,\ln\left(\frac{\rho_{\rm th}}{\rho_{\rm end}}\right) - \frac{1}{12}\,\ln\left(g_{\rm th}\right),$$

where $\rho_{\rm end}$ is the energy density at the end of inflation, $a_0\, H_0$ is the present Hubble scale, $V_\ast$ is the potential energy when $k_\ast$ left the Hubble radius during inflation, and $g_{\rm th}$ is the number of effective bosonic degrees of freedom at the energy scale $\rho_{\rm th}$.

[20] A. R. Liddle and S. M. Leach, Phys. Rev. D **68**, 103503, (2003);
J. Martin and C. Ringeval, Phys. Rev. D **82**, 023511 (2010).

Accounting for post-inflationary evolution

The uncertainties post-inflation are modeled by two parameters: the energy scale $\rho_{\rm th}$ by which the universe has thermalized, and the parameter $w_{\rm int}$ which characterizes the effective equation of state between the end of inflation and the energy scale specified by $\rho_{\rm th}$.

The number of e-folds to the end of inflation is described by the expression[20]

$$N_\ast \approx 67 - \ln\left(\frac{k_\ast}{a_0\, H_0}\right) + \frac{1}{4}\ln\left(\frac{V_\ast^2}{M_{\rm Pl}^4\, \rho_{\rm end}}\right) + \frac{1-3\, w_{\rm int}}{12\, (1+w_{\rm int})}\ln\left(\frac{\rho_{\rm th}}{\rho_{\rm end}}\right) - \frac{1}{12}\ln\left(g_{\rm th}\right),$$

where $\rho_{\rm end}$ is the energy density at the end of inflation, $a_0\, H_0$ is the present Hubble scale, $V_\ast$ is the potential energy when $k_\ast$ left the Hubble radius during inflation, and $g_{\rm th}$ is the number of effective bosonic degrees of freedom at the energy scale $\rho_{\rm th}$.

The Planck team set $k_\ast = 0.002\ {\rm Mpc}^{-1}$, $g_{\rm th} = 10^3$ and a logarithmic prior was chosen on $\rho_{\rm th}$ (in the interval $[(10^3\,{\rm GeV})^4, \rho_{\rm end}]$).

[20] A. R. Liddle and S. M. Leach, Phys. Rev. D **68**, 103503, (2003);
J. Martin and C. Ringeval, Phys. Rev. D **82**, 023511 (2010).

Performance of models in the $n_{\rm s}$-r plane

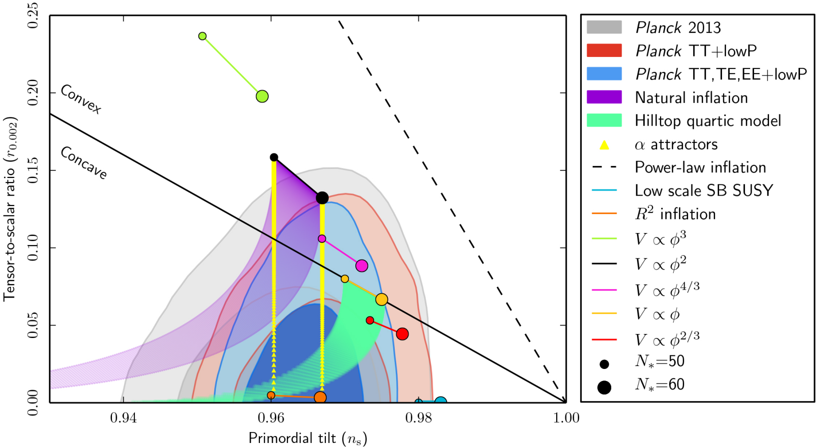

Marginalized joint $68\,\%$ and $95\,\%$ CL regions for $n_{\rm s}$ and $r_{0.002}$ from Planck in combination with other data sets, compared to the theoretical predictions of selected inflationary models[21].

[21] Planck Collaboration (P. A. R. Ade *et al.*), Astron. Astrophys. **594**, A20 (2016).

Likelihood for specific inflationary models

Inflationary model	$\Delta\chi^2$		$\ln B_{0X}$	
	$w_{\rm int}=0$	$w_{\rm int}\neq 0$	$w_{\rm int}=0$	$w_{\rm int}\neq 0$
$R+R^2/(6\,M^2)$	$+0.8$	$+0.3$	$\ldots$	$+0.7$
$n=2/3$	$+6.5$	$+3.5$	-2.4	-2.3
$n=1$	$+6.2$	$+5.5$	-2.1	-1.9
$n=4/3$	$+6.4$	$+5.5$	-2.6	-2.4
$n=2$	$+8.6$	$+8.1$	-4.7	-4.6
$n=3$	$+22.8$	$+21.7$	-11.6	-11.4
$n=4$	$+43.3$	$+41.7$	-23.3	-22.7
Natural	$+7.2$	$+6.5$	-2.4	-2.3
Hilltop ($p=2$)	$+4.4$	$+3.9$	-2.6	-2.4
Hilltop ($p=4$)	$+3.7$	$+3.3$	-2.8	-2.6
Double well	$+5.5$	$+5.3$	-3.1	-2.3
Brane inflation ($p=2$)	$+3.0$	$+2.3$	-0.7	-0.9
Brane inflation ($p=4$)	$+2.8$	$+2.3$	-0.4	-0.6
Exponential inflation	$+0.8$	$+0.3$	-0.7	-0.9
SB SUSY	$+0.7$	$+0.4$	-2.2	-1.7
Supersymmetric α-model	$+0.7$	$+0.1$	-1.8	-2.0
Superconformal ($m=1$)	$+0.9$	$+0.8$	-2.3	-2.2
Superconformal ($m\neq 1$)	$+0.7$	$+0.5$	-2.4	-2.6

The improvement in the likelihood $\Delta\chi^2$ (with respect to the base ΛCDM model) and the Bayes factor (with respect to R^2 inflation) for a set of inflationary models.

Performance of inflationary models

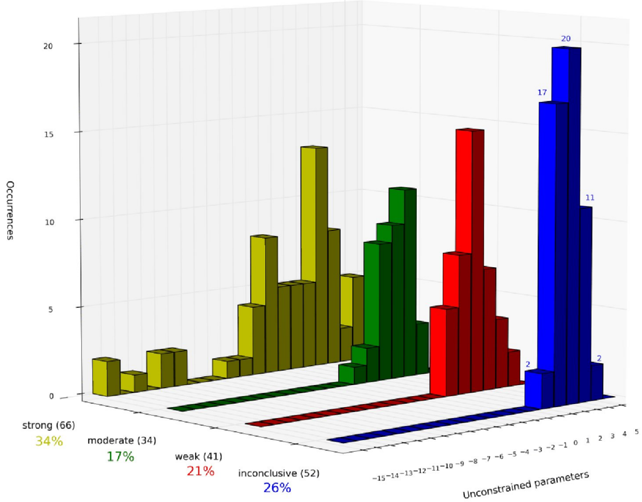

The efficiency of the inflationary paradigm leads to a situation wherein, despite the strong constraints, a variety of models continue to remain consistent with the data[22].

[22] J. Martin, C. Ringeval, R. Trotta and V. Vennin, JCAP **1403**, 039 (2014).

Plan of the talk

Definitions of scalar bispectrum and non-Gaussianity parameter

The scalar bispectrum $\mathcal{B}_{\mathcal{R}\mathcal{R}\mathcal{R}}(\boldsymbol{k}_1, \boldsymbol{k}_2, \boldsymbol{k}_3)$ is related to the three point correlation function of the Fourier modes of the curvature perturbation as follows[23]:

$$\langle \hat{\mathcal{R}}_{\boldsymbol{k}_1}(\eta_{\rm e})\, \hat{\mathcal{R}}_{\boldsymbol{k}_2}(\eta_{\rm e})\, \hat{\mathcal{R}}_{\boldsymbol{k}_3}(\eta_{\rm e})\rangle = (2\,\pi)^3\; \mathcal{B}_{\mathcal{R}\mathcal{R}\mathcal{R}}(\boldsymbol{k}_1, \boldsymbol{k}_2, \boldsymbol{k}_3)\; \delta^{(3)}\left(\boldsymbol{k}_1 + \boldsymbol{k}_2 + \boldsymbol{k}_3\right).$$

[23] D. Larson *et al.*, Astrophys. J. Suppl. **192**, 16 (2011);
E. Komatsu *et al.*, Astrophys. J. Suppl. **192**, 18 (2011).

[24] E. Komatsu and D. N. Spergel, Phys. Rev. D **63**, 063002 (2001).

[25] J. Martin and L. Sriramkumar, JCAP **1201**, 008 (2012).

Definitions of scalar bispectrum and non-Gaussianity parameter

The scalar bispectrum $\mathcal{B}_{\mathcal{R}\mathcal{R}\mathcal{R}}(\boldsymbol{k}_1, \boldsymbol{k}_2, \boldsymbol{k}_3)$ is related to the three point correlation function of the Fourier modes of the curvature perturbation as follows[23]:

$$\langle \hat{\mathcal{R}}_{\boldsymbol{k}_1}(\eta_{\rm e})\, \hat{\mathcal{R}}_{\boldsymbol{k}_2}(\eta_{\rm e})\, \hat{\mathcal{R}}_{\boldsymbol{k}_3}(\eta_{\rm e})\rangle = (2\,\pi)^3\; \mathcal{B}_{\mathcal{R}\mathcal{R}\mathcal{R}}(\boldsymbol{k}_1, \boldsymbol{k}_2, \boldsymbol{k}_3)\; \delta^{(3)}\,(\boldsymbol{k}_1 + \boldsymbol{k}_2 + \boldsymbol{k}_3)\,.$$

The observationally relevant non-Gaussianity parameter $f_{_{\rm NL}}$ is basically introduced through the relation[24]

$$\mathcal{R}(\eta, \boldsymbol{x}) = \mathcal{R}_{_{\rm G}}(\eta, \boldsymbol{x}) - \frac{3\, f_{_{\rm NL}}}{5}\; \left[\mathcal{R}_{_{\rm G}}^2(\eta, \boldsymbol{x}) - \langle \mathcal{R}_{_{\rm G}}^2(\eta, \boldsymbol{x})\rangle\right],$$

where $\mathcal{R}_{_{\rm G}}$ denotes the Gaussian quantity. Utilizing the above relation and Wick's theorem, one can arrive at the following relation[25]:

$$\begin{aligned} f_{_{\rm NL}}(\boldsymbol{k}_1, \boldsymbol{k}_2, \boldsymbol{k}_3) &= -\frac{10}{3}\,(2\,\pi)^{1/2}\; \left(k_1^3\, k_2^3\, k_3^3\right)\; \mathcal{B}_{\mathcal{R}\mathcal{R}\mathcal{R}}(\boldsymbol{k}_1, \boldsymbol{k}_2, \boldsymbol{k}_3) \\ &\quad \times\; \left[k_1^3\; \mathcal{P}_{_{\rm S}}(k_2)\; \mathcal{P}_{_{\rm S}}(k_3) + \text{two permutations}\right]^{-1}. \end{aligned}$$

[23] D. Larson *et al.*, Astrophys. J. Suppl. **192**, 16 (2011);
E. Komatsu *et al.*, Astrophys. J. Suppl. **192**, 18 (2011).

[24] E. Komatsu and D. N. Spergel, Phys. Rev. D **63**, 063002 (2001).

[25] J. Martin and L. Sriramkumar, JCAP **1201**, 008 (2012).

The shape of the slow roll bispectrum

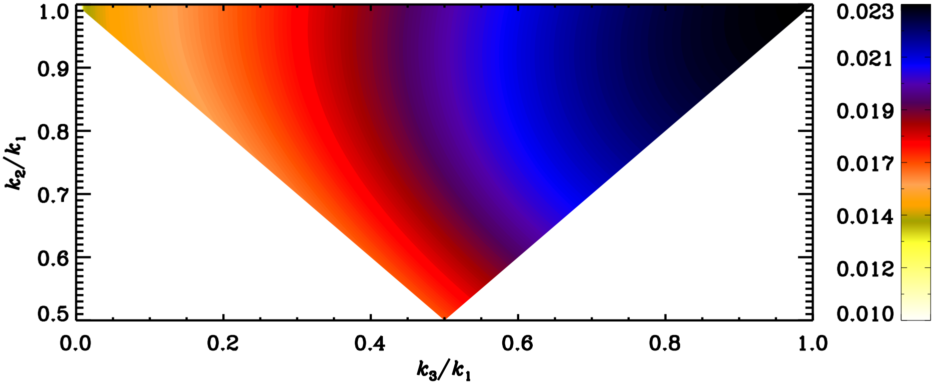

The non-Gaussianity parameter $f_{\rm NL}$, evaluated in the slow roll approximation, has been plotted as a function of k_3/k_1 and k_2/k_1 for the case of the popular quadratic potential. Note that the non-Gaussianity parameter peaks in the equilateral limit wherein $k_1 = k_2 = k_3$. In slow roll scenarios involving the canonical scalar field, the largest value of $f_{\rm NL}$ is found to be of the order of the first slow roll parameter ϵ_1[26].

[26] Figure from D. K. Hazra, L. Sriramkumar and J. Martin, JCAP **1305**, 026, (2013).

Template bispectra

For comparison with the observations, the scalar bispectrum is often expressed in terms of the parameters $f_{\rm NL}^{\rm loc}$, $f_{\rm NL}^{\rm eq}$ and $f_{\rm NL}^{\rm orth}$ as follows:

$$G_{\mathcal{RRR}}(\boldsymbol{k}_1, \boldsymbol{k}_2, \boldsymbol{k}_3) = f_{\rm NL}^{\rm loc}\, G_{\mathcal{RRR}}^{\rm loc}(\boldsymbol{k}_1, \boldsymbol{k}_2, \boldsymbol{k}_3) + f_{\rm NL}^{\rm eq}\, G_{\mathcal{RRR}}^{\rm eq}(\boldsymbol{k}_1, \boldsymbol{k}_2, \boldsymbol{k}_3) + f_{\rm NL}^{\rm orth}\, G_{\mathcal{RRR}}^{\rm orth}(\boldsymbol{k}_1, \boldsymbol{k}_2, \boldsymbol{k}_3).$$

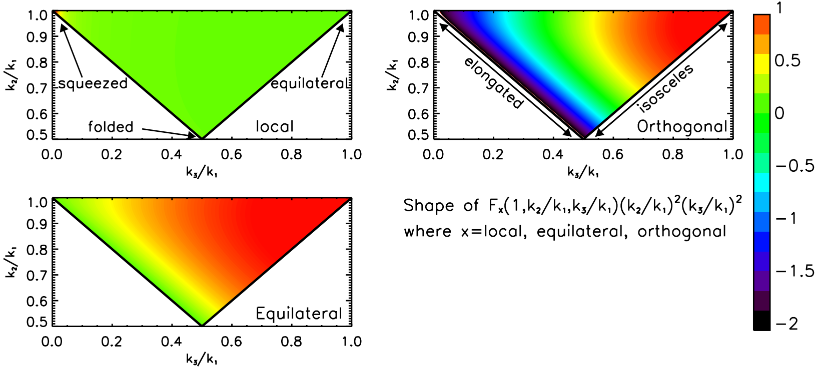

Illustration of the three template basis bispectra[27].

[27] E. Komatsu, Class. Quantum Grav. **27**, 124010 (2010).

Constraints on the scalar non-Gaussianity parameters

The constraints on the primordial values of the non-Gaussianity parameters from the Planck data are as follows[28]:

$$\begin{aligned} f_{\rm NL}^{\rm loc} &= 0.8 \pm 5.0, \\ f_{\rm NL}^{\rm eq} &= -4 \pm 43, \\ f_{\rm NL}^{\rm orth} &= -26 \pm 21. \end{aligned}$$

[28] Planck Collaboration (P. A. R. Ade *et al.*), Astron. Astrophys. **594**, A17 (2016).

Constraints on the scalar non-Gaussianity parameters

The constraints on the primordial values of the non-Gaussianity parameters from the Planck data are as follows[28]:

$$\begin{aligned} f_{\rm NL}^{\rm loc} &= 0.8 \pm 5.0, \\ f_{\rm NL}^{\rm eq} &= -4 \pm 43, \\ f_{\rm NL}^{\rm orth} &= -26 \pm 21. \end{aligned}$$

It should be stressed that these are constraints on the primordial values.

[28] Planck Collaboration (P. A. R. Ade *et al.*), Astron. Astrophys. **594**, A17 (2016).

Constraints on the scalar non-Gaussianity parameters

The constraints on the primordial values of the non-Gaussianity parameters from the Planck data are as follows[28]:

$$
\begin{aligned}
f_{\rm NL}^{\rm loc} &= 0.8 \pm 5.0, \\
f_{\rm NL}^{\rm eq} &= -4 \pm 43, \\
f_{\rm NL}^{\rm orth} &= -26 \pm 21.
\end{aligned}
$$

It should be stressed that these are constraints on the primordial values.

Also, the constraints on each of the $f_{\rm NL}$ parameters have been arrived at assuming that the other two parameters are zero.

[28] Planck Collaboration (P. A. R. Ade *et al.*), Astron. Astrophys. **594**, A17 (2016).

Constraints on the scalar non-Gaussianity parameters

The constraints on the primordial values of the non-Gaussianity parameters from the Planck data are as follows[28]:

$$\begin{aligned} f_{\rm NL}^{\rm loc} &= 0.8 \pm 5.0, \\ f_{\rm NL}^{\rm eq} &= -4 \pm 43, \\ f_{\rm NL}^{\rm orth} &= -26 \pm 21. \end{aligned}$$

It should be stressed that these are constraints on the primordial values.

Also, the constraints on each of the $f_{\rm NL}$ parameters have been arrived at assuming that the other two parameters are zero.

These constraints imply that slowly rolling single field models involving the canonical scalar field which are favored by the data at the level of power spectra are also consistent with the data at the level of non-Gaussianities.

[28] Planck Collaboration (P. A. R. Ade *et al.*), Astron. Astrophys. **594**, A17 (2016).

Plan of the talk

The ‘detection’ of the B-mode polarization by BICEP2

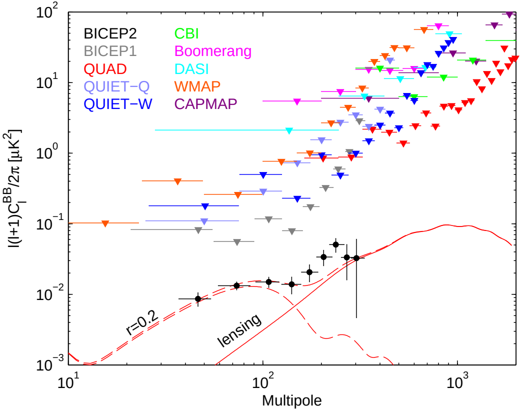

The supposed ‘detection’ of the angular power spectrum of the B-mode polarization of the CMB by BICEP2 as well as the limits that have been arrived at by the earlier efforts[29] The BICEP2 observations, *viz.* the black dots with error bars, had seemed to be consistent with a tensor-to-scalar ratio of $r \simeq 0.2$.

[29] P. A. R. Ade *et al.*, Phys. Rev. Lett. **112**, 241101 (2014)..

Constraints from the BICEP2 data[30]

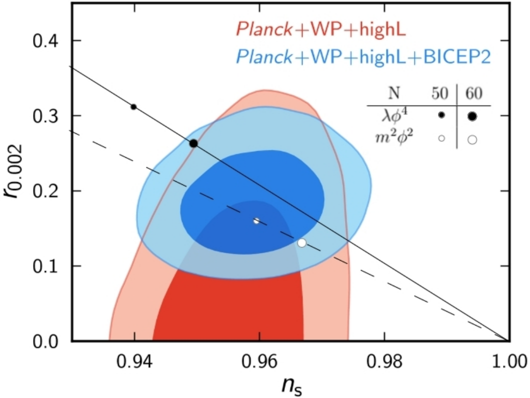

Joint constraints from the BICEP2 observations, the Planck data, the polarization data from WMAP as well as data for the high multipoles from SPT and ACT, on the inflationary parameters $n_{\rm s}$ and r.

[30] P. A. R. Ade *et al.*, arXiv:1403.3985 [astro-ph.CO].

The scale of inflation

During slow roll, if we ignore the weak scale dependence, we can write

$$r \simeq \frac{2\,V}{3\,\pi^2\,M_{\rm Pl}^4}\,\frac{1}{\mathcal{A}_{\rm S}},$$

where, recall that, $\mathcal{A}_{\rm S}$ denotes the amplitude of the scalar perturbations.

The amplitude of the primordial scalar perturbations is usually quoted at the pivot scales of either 0.05 or $0.02\ {\rm Mpc}^{-1}$, which correspond to multipoles that lie in the Sachs-Wolfe plateau. This value for the scalar amplitude is often referred to as COBE normalization[31].

According to COBE normalization, $\mathcal{A}_{\rm S} \simeq 2.14 \times 10^{-9}$, which implies that we can write

$$V^{1/4} \simeq 3.2 \times 10^{16}\, r^{1/4}\ {\rm GeV} \simeq 2.1 \times 10^{16}\ {\rm GeV},$$

with the final value being for the case wherein $r \simeq 0.2$.

Note that, if $H_{\rm I}$ represents the Hubble scale during the inflationary epoch, as $H_{\rm I}^2 \simeq V/(3\,M_{\rm Pl}^2)$ during slow roll, the above relation also leads to

$$\frac{H_{\rm I}}{M_{\rm Pl}} \simeq 4.6 \times 10^{-5}.$$

[31] E. F. Bunn, A. R. Liddle and M. J. White, Phys. Rev. D **54**, R5917 (1996).

Models with small tensor-to-scalar ratio

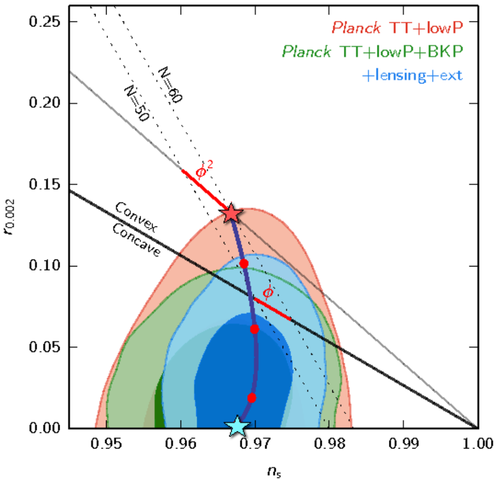

The theorists are ahead! The so-called alpha-attractor models which can lead to rather small values of the tensor-to-scalar ratio[32].

[32] R. Kallosh and A. Linde, Phys. Rev. D **91**, 083528 (2015).

The n_s-r-plane with CORE

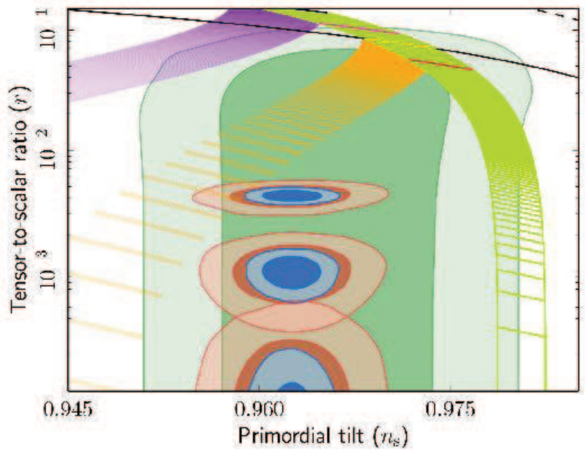

Marginalized forecasts for CORE[33]. The small blue contours illustrate what a CORE detection would look like if $r \simeq 0.0042$ (as in the Starobinsky model), $r \simeq 0.001$ or when the tensors are undetectably small. The red contours correspond to forecasts for LITEBIRD.

[33] F. Finelli *et al.*, arXiv:1612.08270 [astro-ph.CO].

CORE forecasts for the slow roll consistency relation

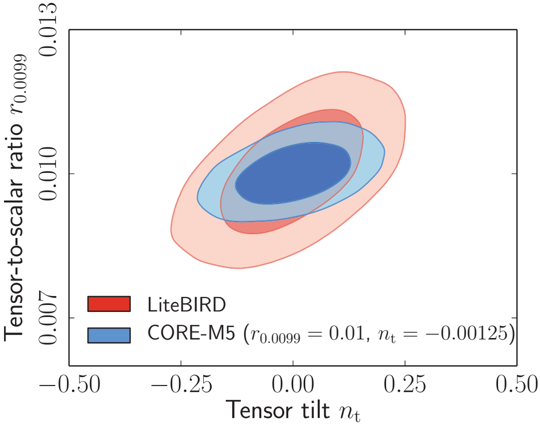

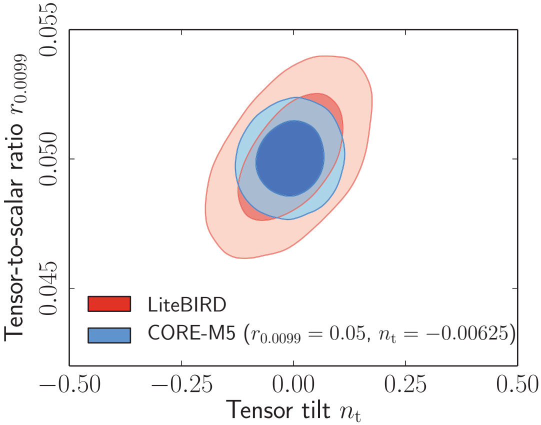

Marginalized forecasts for the slow roll consistency relation corresponding to two different values of the tensor-to-scalar ratio [34]. Deviations from the consistency relation would imply inflation driven by multiple fields.

[34] F. Finelli *et al.*, arXiv:1612.08270 [astro-ph.CO].

Discriminating between different post-inflationary dynamics

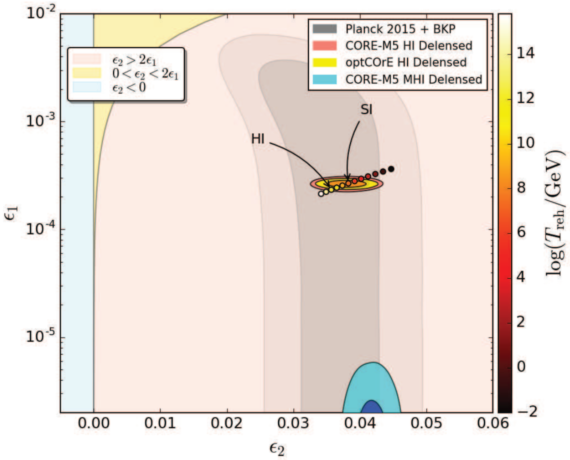

Marginalized forecasts for CORE[35]. CORE can, in principle, distinguish between Higgs inflation (HI) and Starobinsky inflation (SI), which share the same inflationary potential, but have different reheating temperatures (around $10^{12}\,\mathrm{GeV}$ for HI and $10^{8}\,\mathrm{GeV}$ for SI).

[35] F. Finelli *et al.*, arXiv:1612.08270 [astro-ph.CO].

Introducing additional non-Gaussianity parameters

Extending the original argument for introducing the parameter $f_{_{\rm NL}}$, one can introduce dimensionless non-Gaussianity parameters, say, $C_{_{\rm NL}}^{\mathcal{R}}$, $C_{_{\rm NL}}^{\gamma}$ and $h_{_{\rm NL}}$, to characterize the three-point functions involving tensors as follows[36]:

$$\begin{aligned}\mathcal{R}(\eta,\boldsymbol{x}) &= \mathcal{R}_{_{\rm G}}(\eta,\boldsymbol{x}) - \frac{3\,f_{_{\rm NL}}}{5}\,\left[\mathcal{R}_{_{\rm G}}^2(\eta,\boldsymbol{x}) - \langle\mathcal{R}_{_{\rm G}}^2(\eta,\boldsymbol{x})\rangle\right]\\ &\quad - C_{_{\rm NL}}^{\mathcal{R}}\,\mathcal{R}_{_{\rm G}}(\eta,\boldsymbol{x})\,\gamma_{\bar{m}\bar{n}}^{\rm G}(\eta,\boldsymbol{x})\end{aligned}$$

and

$$\begin{aligned}\gamma_{ij}(\eta,\boldsymbol{x}) &= \gamma_{ij}^{\rm G}(\eta,\boldsymbol{x}) - h_{_{\rm NL}}\,\left[\gamma_{ij}^{\rm G}(\eta,\boldsymbol{x})\,\gamma_{\bar{m}\bar{n}}^{\rm G}(\eta,\boldsymbol{x}) - \langle\gamma_{ij}^{\rm G}(\eta,\boldsymbol{x})\,\gamma_{\bar{m}\bar{n}}^{\rm G}(\eta,\boldsymbol{x})\rangle\right]\\ &\quad - C_{_{\rm NL}}^{\gamma}\,\gamma_{ij}^{\rm G}(\eta,\boldsymbol{x})\,\mathcal{R}_{_{\rm G}}(\eta,\boldsymbol{x}),\end{aligned}$$

where $\mathcal{R}_{_{\rm G}}$ and $\gamma_{ij}^{\rm G}$ denote the Gaussian quantities.

[36] V. Sreenath, R. Tibrewala and L. Sriramkumar, JCAP **1312**, 037 (2013).

Expressions describing the non-Gaussianity parameters

One finds that the non-Gaussianity parameters $C_{_{\rm NL}}^{\mathcal{R}}$, $C_{_{\rm NL}}^{\gamma}$ and $h_{_{\rm NL}}$ can be expressed in terms of the scalar-scalar-tensor and the scalar-tensor-tensor cross-correlations and the tensor bispectrum as[37]

$$
\begin{aligned}
C_{_{\rm NL}}^{\mathcal{R}} &= -\frac{4}{(2\,\pi^2)^2}\,\left[k_1^3\,k_2^3\,k_3^3\;G_{\mathcal{R}\mathcal{R}\gamma}^{m_3n_3}(\boldsymbol{k}_1,\boldsymbol{k}_2,\boldsymbol{k}_3)\right]\\
&\quad\times\left(\Pi^{\boldsymbol{k}_3}_{m_3n_3,\bar{m}\bar{n}}\right)^{-1}\,\left\{\left[k_1^3\,\mathcal{P}_{_{\rm S}}(k_2)+k_2^3\,\mathcal{P}_{_{\rm S}}(k_1)\right]\,\mathcal{P}_{_{\rm T}}(k_3)\right\}^{-1},\\
C_{_{\rm NL}}^{\gamma} &= -\frac{4}{(2\,\pi^2)^2}\,\left[k_1^3\,k_2^3\,k_3^3\;G_{\mathcal{R}\gamma\gamma}^{m_2n_2m_3n_3}(\boldsymbol{k}_1,\boldsymbol{k}_2,\boldsymbol{k}_3)\right]\\
&\quad\times\left\{\mathcal{P}_{_{\rm S}}(k_1)\,\left[\Pi^{\boldsymbol{k}_2}_{m_2n_2,m_3n_3}\,k_3^3\,\mathcal{P}_{_{\rm T}}(k_2)+\Pi^{\boldsymbol{k}_3}_{m_3n_3,m_2n_2}\,k_2^3\,\mathcal{P}_{_{\rm T}}(k_3)\right]\right\}^{-1},\\
h_{_{\rm NL}} &= -\left(\frac{4}{2\,\pi^2}\right)^2\,\left[k_1^3\,k_2^3\,k_3^3\;G_{\gamma\gamma\gamma}^{m_1n_1m_2n_2m_3n_3}(\boldsymbol{k}_1,\boldsymbol{k}_2,\boldsymbol{k}_3)\right]\\
&\quad\times\left[\Pi^{\boldsymbol{k}_1}_{m_1n_1,m_2n_2}\,\Pi^{\boldsymbol{k}_2}_{m_3n_3,\bar{m}\bar{n}}\,k_3^3\,\mathcal{P}_{_{\rm T}}(k_1)\,\mathcal{P}_{_{\rm T}}(k_2)+\text{five permutations}\right]^{-1}.
\end{aligned}
$$

[37] V. Sreenath, R. Tibrewala and L. Sriramkumar, JCAP **1312**, 037 (2013).

The shapes of the additional non-Gaussianity parameters

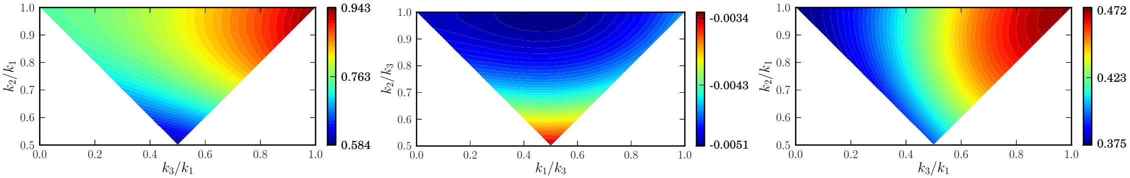

The shapes of the non-Gaussianity parameters involving the tensor perturbations $C_{\rm NL}^{\mathcal{R}}$ (on the left), $C_{\rm NL}^{\gamma}$ (in the middle) and $h_{\rm NL}$ (on the right) in the case of the standard quadratic potential leading to slow roll inflation[38].

[38] V. Sreenath, R. Tibrewala and L. Sriramkumar, JCAP **1312**, 037 (2013).

Constraints on $h_{\rm NL}$

The Planck observations have led to the following constraint on the $h_{\rm NL}$ parameter[39]:

$$h_{\rm NL} = (4 \pm 15) \times 10^2.$$

[39] Planck Collaboration (P. A. R. Ade *et al.*), Astron. Astrophys. **594**, A20 (2016).

Plan of the talk

Power spectra with features

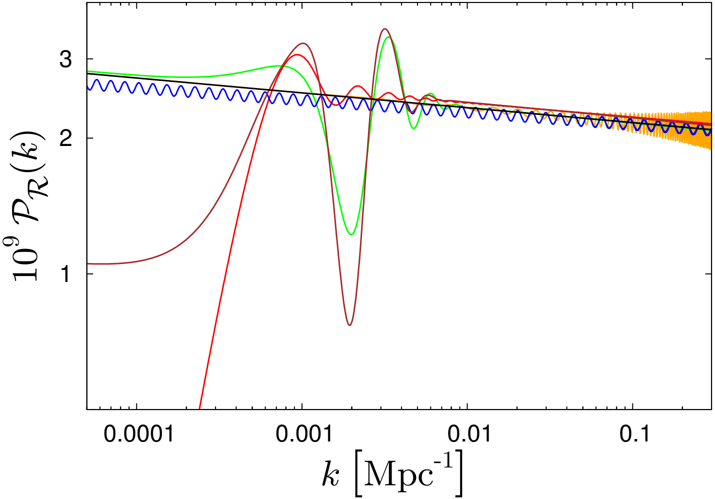

Primordial power spectra with features that lead to an improved fit to the data than the conventional, nearly scale, invariant spectra[40].

[40] Planck Collaboration (P. A. R. Ade *et al.*), Astron. Astrophys. **594**, A20 (2016).

Inflationary models permitting deviations from slow roll

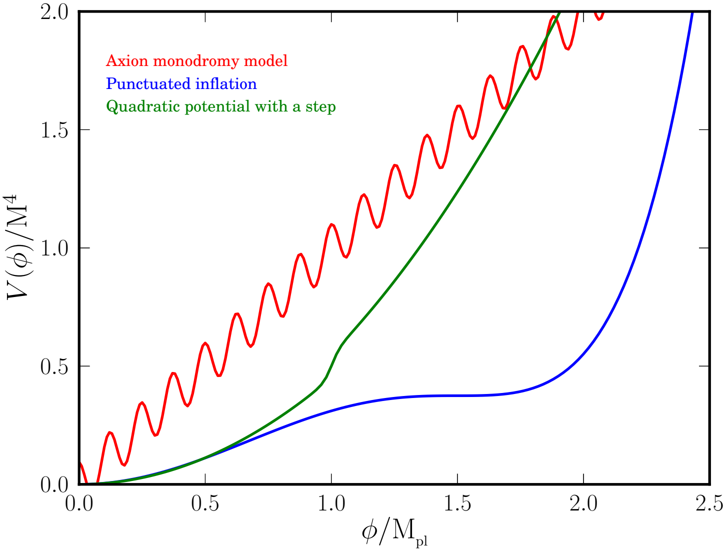

Illustration of potentials that admit departures from slow roll.

Spectra leading to an improved fit to the CMB data

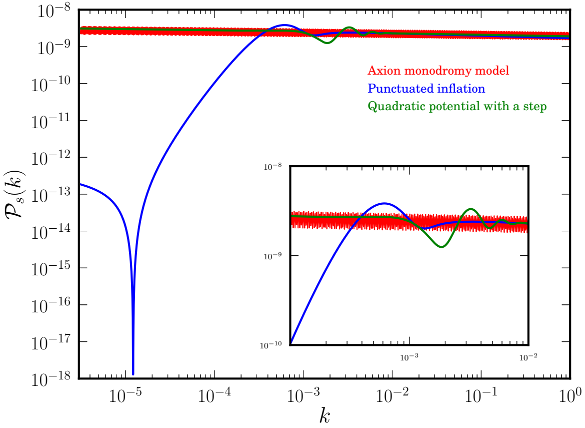

The scalar power spectra in different inflationary models that lead to a better fit to the CMB data than the conventional power law spectrum[41].

[41] R. K. Jain, P. Chingangbam, J.-O. Gong, L. Sriramkumar and T. Souradeep, JCAP **0901**, 009 (2009); D. K. Hazra, M. Aich, R. K. Jain, L. Sriramkumar and T. Souradeep, JCAP **1010**, 008 (2010); M. Aich, D. K. Hazra, L. Sriramkumar and T. Souradeep, Phys. Rev. D **87**, 083526 (2013).

$f_{\rm NL}$ in models with features

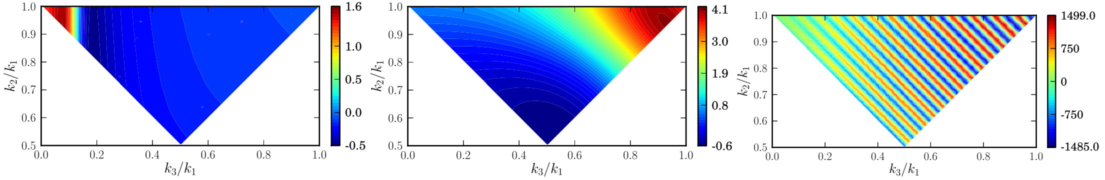

The scalar non-Gaussianity parameter $f_{\rm NL}$ in the punctuated inflationary scenario (on the left), quadratic potential with a step (in the middle) and the axion monodromy model (on the right), evaluated using BINGO[42].

[42] D. K. Hazra, L. Sriramkumar and J. Martin, JCAP **1305**, 026 (2013).

The inflationary scalar bispectrum

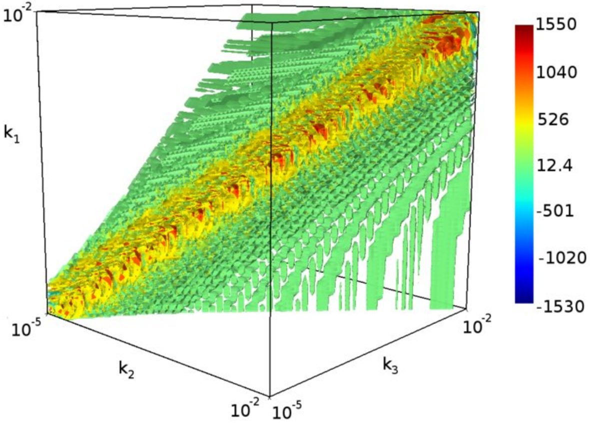

The complete shape of the inflationary scalar bispectrum (actually, the non-Gaussianity parameter $f_{\rm NL}$) in the case of the axion monodromy model[43].

[43] V. Sreenath, D. K. Hazra and L. Sriramkumar, JCAP **1502**, 029 (2015).

Consistency relations away from slow roll

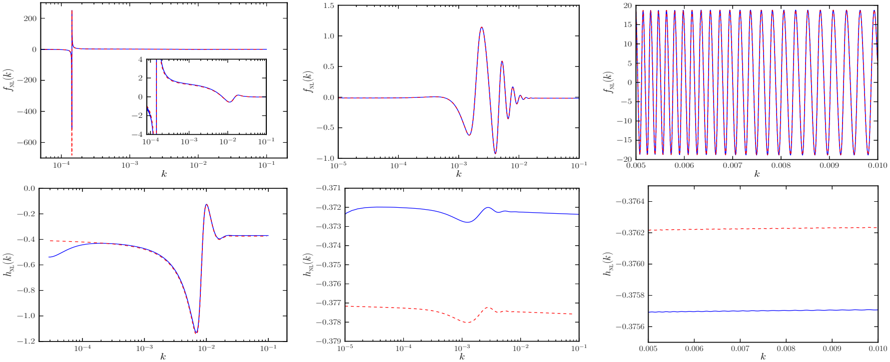

The behavior of the quantities $f_{\rm NL}$ (on top) and $h_{\rm NL}$ (at the bottom) in the squeezed limit has been plotted as a function of the wavenumber in the case of the punctuated inflationary scenario (on the left), the quadratic potential with a step (in the middle) and the axion monodromy model (on the right). The solid blue curves represent the numerical results obtained from the three-point functions, while the red dashed curves denote those arrived at using the consistency relations[44].

[44] V. Sreenath, D. K. Hazra and L. Sriramkumar, JCAP **1502**, 029 (2015); V. Sreenath and L. Sriramkumar, JCAP 1410, 021 (2014).

Reconstruction of primordial spectra with features

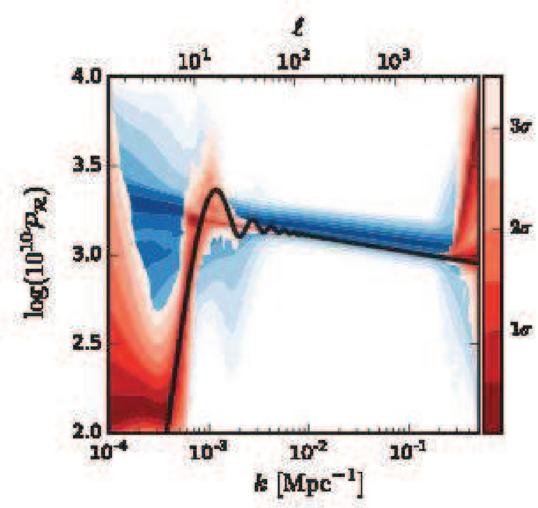

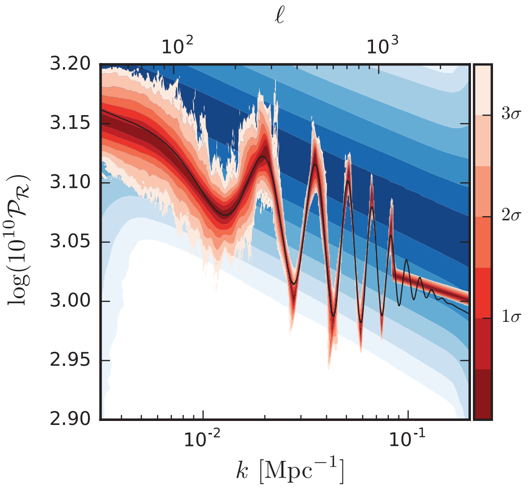

Reconstructing a simulated power spectrum with features (black lines) for a CORE experiment (in red), compared to existing constraints provided by Planck (in blue)[45].

[45] F. Finelli *et al.*, arXiv:1612.08270 [astro-ph.CO].

Plan of the talk

Summary: The inflationary scenario

- A nearly scale invariant primordial spectrum as is generated in slow roll inflation is remarkably consistent with the cosmological data.

[46] J. Martin, C. Ringeval and V. Vennin, Phys. Dark Univ. **5–6**, 75 (2014).
[47] J. R. Fergusson, H. F. Gruetjen, E. P. S. Shellard and M. Liguori, Phys. Rev. D **91**, 023502 (2015).

Summary: The inflationary scenario

- A nearly scale invariant primordial spectrum as is generated in slow roll inflation is remarkably consistent with the cosmological data.
- The strong constraints on the scalar non-Gaussianity parameter seem to further support slow roll models of inflation.

[46] J. Martin, C. Ringeval and V. Vennin, Phys. Dark Univ. **5–6**, 75 (2014).

[47] J. R. Fergusson, H. F. Gruetjen, E. P. S. Shellard and M. Liguori, Phys. Rev. D **91**, 023502 (2015).

Summary: The inflationary scenario

- A nearly scale invariant primordial spectrum as is generated in slow roll inflation is remarkably consistent with the cosmological data.
- The strong constraints on the scalar non-Gaussianity parameter seem to further support slow roll models of inflation.
- While there exist some anomalies (features in the power spectra, hemispherical asymmetry, etc.), they do not seem to have substantial statistical significance.

[46] J. Martin, C. Ringeval and V. Vennin, Phys. Dark Univ. **5–6**, 75 (2014).

[47] J. R. Fergusson, H. F. Gruetjen, E. P. S. Shellard and M. Liguori, Phys. Rev. D **91**, 023502 (2015).

Summary: The inflationary scenario

- A nearly scale invariant primordial spectrum as is generated in slow roll inflation is remarkably consistent with the cosmological data.
- The strong constraints on the scalar non-Gaussianity parameter seem to further support slow roll models of inflation.
- While there exist some anomalies (features in the power spectra, hemispherical asymmetry, etc.), they do not seem to have substantial statistical significance.
- One may need to carry out a systematic search involving the scalar and the tensor power spectra[46], the scalar and the tensor bispectra and the cross correlations to arrive at a smaller subset of viable inflationary models[47].

[46] J. Martin, C. Ringeval and V. Vennin, Phys. Dark Univ. **5–6**, 75 (2014).

[47] J. R. Fergusson, H. F. Gruetjen, E. P. S. Shellard and M. Liguori, Phys. Rev. D **91**, 023502 (2015).

Outlook: The difficulty with the inflationary paradigm

So even before the Planck satellite flies we can rest assured that a single field inflation model will match almost any possible observation of the scalar and tensor power spectra![a]

[a] From E. P. S. Shellard, *The future of cosmology: Observational and computational prospects*, in *The Future of Theoretical Physics and Cosmology*, Eds. G. W. Gibbons, E. P. S. Shellard and S. J. Rankin (Cambridge University Press, Cambridge, England, 2003).

A theory that predicts everything predicts nothing[a].

[a] P. J. Steinhardt, Sci. Am. **304**, 36 (2011).

Thank you for your attention